Multiplet cascade in a semiconductor laser with optoelectronic feedback

Md Shariful Islam, A. Kovalev, G. Danilenko, E. Viktorov, D. Citrin, Alexandre Locquet

Multiplet Cascade in a Semiconductor Laser with Optoelectronic Feedback

Md Shariful Islam,[1,2] A. V. Kovalev,[3] G. O. Danilenko,[3] E. A. Viktorov,[3] D. S. Citrin,[4,2] and A. Locquet[4,2]
[1)] *Georgia Tech-CNRS IRL 2958, Georgia Tech-Europe, 2 Rue Marconi, 57070 Metz, France*
[2)] *School of Electrical and Computer Engineering, Georgia Institute of Technology, Atlanta,Georgia 30332-0250, USA*
[3)] *ITMO University, Birzhevaya Liniya 14, 199034 Saint Petersburg, Russia*
[4)] *Georgia Tech-CNRS IRL 2958, Georgia Tech Europe, 2 Rue Marconi, 57070 Metz, France*

(*Electronic mail: avkovalev@itmo.ru)

(Dated: 24 September 2024)

We report experimentally and theoretically a dynamical scenario involving the formation of pulse multiplet structures, *i.e.*, configurations of two, three, and more pulses per roundtrip, in a semiconductor laser with positive optoelectronic feedback. The delayed feedback loop includes a cascade of two band-limited amplifiers with nonlinear saturation of sigmoid type. The multiplets appear subcritically in the vicinity of the lasing threshold, resembling gain-switched operation, and evolve with the injection current.

Bursting dynamics are widespread in chemical and biological systems, and have attracted significant interest in neuroscience[1]. In laser physics, a bursting mode in high power lasers in the form of time periodic regular nonequidistant pulsations of the laser output has been observed and has been used to increase the rate of laser ablation[2,3], and, in particular, micro-drilling[4,5], high-speed imaging[6], and distance measurements[7]. Typically, the bursting regime in high power lasers is achieved by either Q-switching or cavity dumping and can employ additional amplification for higher pulse energy. In semiconductor lasers, by contrast, the bursts of pulses can be obtained by using optical injection in combination with gain-switched operation[8], or in a dual-state quantum-dot laser[9]. Passively mode-locked pulses can also be transformed into bursts of pulses also known as lasing localized structures[10]. Symmetry-broken states of pulsations have recently been considered in a semiconductor laser with a saturable absorber and incoherent delayed feedback[11].

Gain-switching is a well established technique to generate pulsations from semiconductor lasers[12] with applications in microwave photonics[13,14] and integrated soliton microcombs[15]. A gain-switching mechanism can be achieved around the laser injection threshold (J_{th}) utilising positive optoelectronic (OE) feedback where the current from the OE loop is added back to the injection current (J), resulting in pulsations[16] and rich nonlinear dynamics[17]. Self-pulsing of a quantum dot-based, monolithically integrated microlaser-microdetector assembly with on-chip optoelectronic feedback was reported in Ref. 18, and was addressed to the thermal effects in the gain medium. However, gain-switching with semiconductor lasers is relatively sparsely explored compared to the region of undamped relaxation oscillations that appear well above J_{th}[19]. As can be seen from the extensive work on the latter with both positive and negative OE feedback, in which numerous subharmonic and frequency-locked states have been explored, the wide range of applications of this technology, particularly in optical communications, is evident[20–24].

In this Letter, we experimentally and theoretically consider a semiconductor laser with a filtered *positive* OE feedback containing nonlinear saturation in the electronic part of the loop. We observe a regime of delay-periodic multiplets around the lasing threshold which is intrinsically interesting for studying their rich nonlinear dynamics as well as to obtain a new type of optical pulse train. We identify the physical mechanism underlying the initial formation of multiplets based on a model previously used to describe optical square-wave generation and accounting for filtering and nonlinear saturation in the delayed OE feedback loop[25]. The pulse multiplets with tailored pulsed dynamics explored here are of interest for use, e.g., in a regenerative memory[26] and spiking encoding[27] for neuromorphic data processing, as a bursting illumination laser in high-accuracy lidars[28], and as master oscillator sources in burst-seeded MOPA (Master Oscillator Power Amplifier) configuration[29].

A telecom laser diode (LD) operating at 1550 nm with anti-reflection coated front facet and low beam divergence is used for the experiment. The edge-emitting single-mode DFB structure is based on InGaAsP/InP strained-layer multiple quantum wells. This unpackaged LD is convenient for measuring and modulating the injection terminal voltage at a high frequency by an external signal source or optoelectonic feedback. The LD is thermally stabilized (Thorlabs TED200C) and driven by a regulated current source (Thorlabs LDC201CU). The external slope efficiency, defined as the change in light output per unit of J above J_{th}, is 0.22 mW/mA, where J_{th} is ~ 20 mA for the free-running LD at room temperature. The time-delayed OE feedback modifies the threshold based on the level and sign of the feedback signal. We observe the formation of multiplets in the vicinity of the free-running threshold value.

To construct the OE feedback loop, the LD output passes through a 50/50 beam splitter (BS). One output from the BS goes to a photodetector (PD), with an optical isolator to block back reflections into the LD. The other BS output, leads to an optical spectrum analyzer. The feedback strength is controlled by attenuating the beam before the PD. The feedback strength is measured as the ratio between the root-mean-squared value of the current fed back and the laser injection current (see Ref. 17 for details). In this work, the attenuation was fixed,

and the resulting feedback strength was about 20% for the operation regime where multiplets are detected, analyzed in this paper.

The output of the PD is amplified with a cascade of two 30-dB amplifiers (Microsemi UA0L30VM, 100 kHz–30 GHz) followed by a 12-dB attenuator (Minicircuts BW-S6W2+, DC-18 GHz) before heading to the LD injection terminals through the bias tee (BT, 10 MHz–26.5 GHz bandwidth). Of note, the amplifiers function within a range in which saturable nonlinearity is experienced, *i.e.*, they clip the amplitude of the feedback signal once the input signal surpasses the saturation point. The attenuator placed after the amplifier cascade serves to limit the intensity of the feedback signal to a level that prevents damaging the LD. The DC-arm of the BT is fed by J, and the feedback signal feeds the AC-arm. The electrical signal is measured with an oscilloscope (12-GHz bandwidth, 40 GSa/s) after the PD. The low-noise amplifier in the PD is inverting as well as the two 30-dB amplifiers in the electronic portion of the OE feedback loop, constituting a net negative feedback signal. The LD architecture is anode grounded which leads to an overall *positive* sign of the feedback since injection-terminal voltage as well as the feedback signal have the same polarity. The overall delay τ in the OE loop is 33.64 ns. The delay is measured by directly injecting a square pulse from an external source through the AC-arm of BT and monitoring the output at the end of the electronic branch under open-loop conditions. The upper cut-off frequency of the OE loop is limited to 12 GHz by the PD and the lower cut-off frequency is set by the BT to 10 MHz. The Microsemi amplifiers have a saturated output power rating of 23 dBm. Please refer to Ref. 30 for the experimental setup details and device model numbers.

Figure 1 shows intensity time-series of the PD voltage signal, that is proportional to the LD intensity, for increasing values of J near $J_{\rm th}$. Starting at $J = 19.40$ mA, slightly below $J_{\rm th} = 20$ mA, the system pulses with the repetition time $\tau = 33.64$ ns. The process of pulsing below the J_{th} is due to gain switching induced by the optoelectronic feedback[16,31–33].

At the lower end of the J range shown, pulsing begins with isolated single pulses spaced by time τ, corresponding to a repetition rate of $f_\tau = 1/\tau$. These pulsations are a consequence of self-modulation induced by feedback on the injection current J, and are referred to as gain-switched pulses[30]. As J gradually increases, a doublet pattern develops, as illustrated in Fig. 1(b), transitioning from a single-pulse train, at the same repetition rate f_τ, with a 3.67 ns interval in-between the doublet pulses. With a continuous increase in J, the pulse count rises in integer steps, as evidenced by the appearance of three pulses (triplet) in Fig. 1(c) and four (quadruplet) in Fig. 1(d). A close examination of consecutive time traces reveals that within a multiplet structure, each newly emerged pulse tends to drift further from its predecessor as J increases, and remains within a range of 6.7 ns. Additional increase in J results in the generation of new pulses within the multiplet. As J decreases, a hysteresis effect is observed, and the J values of the corresponding multiplet sequence change. We illustrate the multistable character of the multiplets in Fig. 1(a) where the singlet at $J = 19.60$ mA coexists with the doublet which is

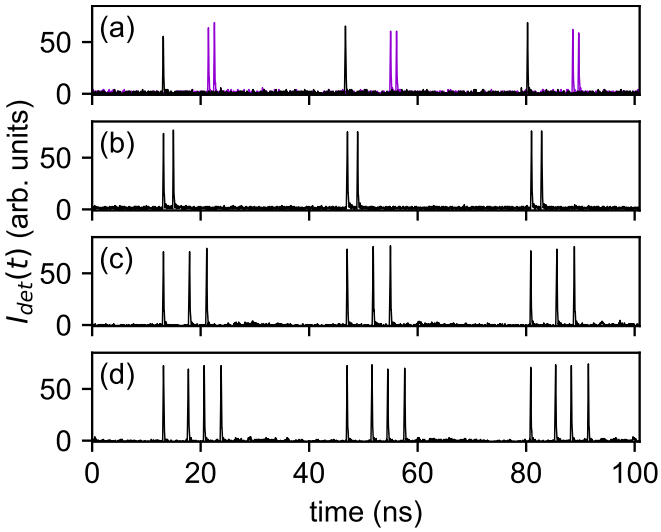

FIG. 1. Time traces of the PD voltage signal $I_{det}(t)$ proportional to the LD intensity as injection current J increases (top to bottom panel). At the lower values of J shown, pulsing at a repetition rate f_τ is observed. As J increases, multiplets (doublets, triplets, ...) form with increasing numbers of pulses per multiplet. The repetition rate between multiplets remains at f_τ. (a) singlet, $J = 19.60$ mA, (b) doublet, $J = 20.40$ mA, (c) triplet, $J = 22.00$ mA, (d) quadruplet, $J = 22.20$ mA. In (a) the singlet (black line) coexists with the doublet (violet line) where the latter is obtained with the decrease in J.

obtained with the decrease in J. We have observed up to seven pulses in a single multiplet before the time series intermittently loses its periodic nature. The multiplets eventually turn into a regular pulsing dominated by the relaxation-oscillation frequency (as in Ref. 17) after a range of aperiodicity. Note that, at $J \gtrsim 2.2 J_{th}$, optical square waves appear, with their period being guided by the feedback delay τ[25].

To theoretically reproduce the experimental results, we use a model of a semiconductor laser subject to filtered nonlinear feedback that was introduced in Ref. 25,

$$\dot{I}_C(t) = 2N(t)I_C(t) + \beta(t), \tag{1}$$

$$\dot{I}_{FH,i}(t) = -{\tau_H}^{-1} I_{FH,i}(t) + \dot{I}_{FH,i-1}(t), \tag{2}$$

$$\dot{I}_{FL,j}(t) = -{\tau_L}^{-1}(I_{FL,j}(t) - I_{FL,j-1}(t)), \tag{3}$$

$$\varepsilon^{-1}\dot{N}(t) = P + s\tanh(k\eta I_{FL,M}(t-\tau)) - N(t) - (1+2N(t))I_C(t). \tag{4}$$

The dot means differentiation with respect to time t, that is in units of the cavity photon lifetime τ_{ph}. $I_C(t)$ is the normalized intracavity intensity of the laser field; $N(t)$ is the normalized carrier density; ε is the ratio of the photon and carrier lifetimes; $\beta(t)$ is a white Gaussian noise source accounting for spontaneous emission with a variance of 10^{-10}; $P = (J/J_{th} - 1)/2$ is the pump parameter relating the injection current J to its threshold value J_{th}. Equations (2)-(3) describe multiple high- and low-pass filters in the feedback loop. $I_{FH,i}(t)$ ($I_{FL,j}(t)$) is the filtered electric signal after the high- (low-) pass filter, $i = 1...K$ ($j = 1...M$) account for the K-th (M-th) stage high- (low-) pass filtering ($I_{FH,0}(t) = I_C(t)$,

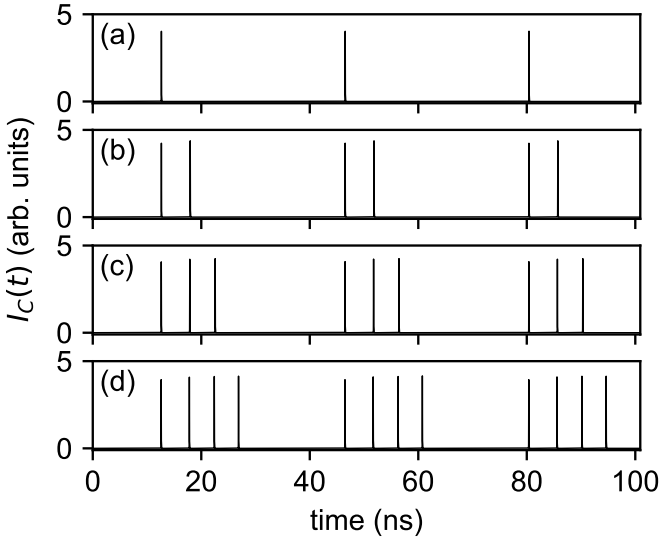

FIG. 2. Theoretical intensity time traces: (a) singlet at $P = -0.01$; (b) doublet at $P = -0.009$; (c) triplet at $P = -0.009$, coexisting with the doublet in (b); (d) quadruplet at $P = -0.0085$. $\eta = 0.00129$, and the other parameters are given in the text.

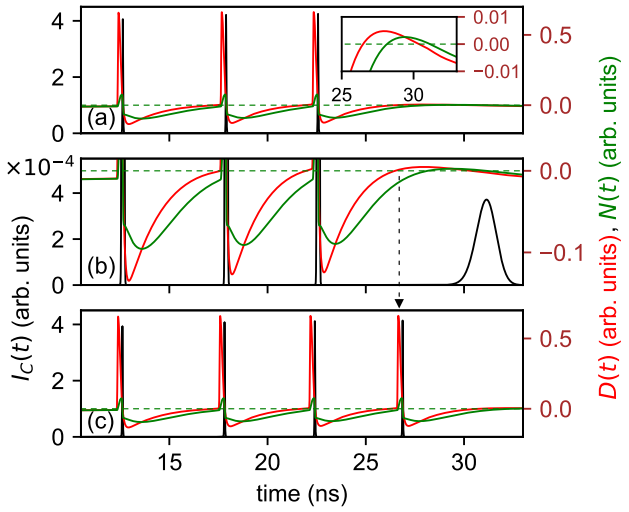

FIG. 3. Detailed theoretical time traces of a triplet (a, b) at $P = -0.009$ and quadruplet (c) at $P = -0.0085$, that correspond to the enlarged traces in Fig. 2(c) and (d), accordingly. The black lines with the scale on the left axis show the intracavity intensity $I_C(t)$. The red and green lines with the scale on the right axis show the driving term, that is sum of the pump and the feedback, $D(t) = P + s\tanh(k\eta I_{FL,1}(t-\tau))$, and the carrier density $N(t)$, respectively. Dashed green line shows the threshold condition for the carrier density, $N(t) = 0$, and inset in the panel (a) shows the area where the threshold becomes exceeded. The panel (b) displays the version of panel (a) with both vertical axes zoomed-in. $\eta = 0.00129$, and the other parameters are given in the text. The arrow between panels (b) and (c) indicates the added pulse position in the quadruplet in the vicinity of the condition $D(t) > 0$ in the triplet.

$I_{FL,0}(t) = I_{FH,K}(t)$), and τ_H (τ_L) is the inverse of the cut-off frequency of the corresponding high- (low-) pass filter.

Nonlinearity of the feedback caused by the amplifiers saturation is accounted by the term $s\tanh[k\eta I_{FL,n}(t-\tau)]$ in Eq. (4) where η represents the feedback level, *i.e.*, the coefficient of the intensity conversion to an electrical signal. k is a small-signal amplification coefficient, and s defines the maximum amplitude of the feedback signal. The feedback is close-to-linear for small feedback level η, and when the signal amplitude is large, the term saturates with its value limited by s. Semiconductor laser time scales are fast and the delayed feedback is slow, and the overall arrangement is, therefore, reminiscent of a typical slow-fast neuromorphic system with a sigmoid-like activation function.

The following parameters are used for the modelling that were chosen to match experimental results: $\tau_{ph} = 1.26$ ps, $\varepsilon = 0.00126$, $\tau = 33.64$ ns, $s = 0.7$, $k = 1000/0.7$, $K = 4$, $M = 1$, $1/\tau_H = 240$ MHz, and $1/\tau_L = 10$ GHz. These parameters define very different time scales, resulting in a stiff system, that was integrated numerically. The numerical time series of the multiplets cascade are shown in Fig. 2 and demonstrate correspondence with the experimental measurements in Fig. 1.

The multiplets form subcritically in the vicinity of the threshold due to the nonlinarity of the gain, and correspond to self-sustained gain-switched pulsations. The electrical signal of the detected laser pulse propagating through the feedback loop is filtered and becomes broader due to the filtration and nonlinear amplification. The amplified regenerative feedback leads to the stable pulsations at a frequency close to the feedback repetition rate f_τ. Figure 3 shows the detailed time traces of the laser intensity $I_C(t)$ and the driving term $D(t) = P + s\tanh(k\eta I_{FL,1}(t-\tau))$ (note the broader pulses of $D(t)$ compared to $I_C(t)$ which resemble the filter impulse response, since the excitation $I_C(t)$ is short) for the triplet at $P = -0.009$ (Fig. 3(a, b)) and the quadruplet at $P = -0.0085$ (Fig. 3(c)). We note here that the theoretical pulses are shorter and relate the difference to the complexities of the multiple bandwidth-limited filters in the experimental loop, and the coupling between the phase and the carriers in a semiconductor laser, which are not accounted for in the modelling. The phase-amplitude coupling, conventionally modelled by the linewidth enhancement factor, may lead to the asymmetry in the pulse profile, and, therefore, to pulse broadening.

The recovery time scale of $D(t)$ is strongly dependent on the high-pass filter cut-off frequency defined by $1/\tau_H$. The multiple-stage high-pass filtering produces ringing as an impulse response of the whole feedback loop, and brings about a pronounced undershoot in the $D(t)$ signal that pulls the carrier density below the threshold, and then an overshoot with a maximum having a positive sign. Its overall impact on the laser dynamics is, therefore, different from that of the filtered optical feedback in Ref. 34, which imposes some limitations on the coupling between the various external cavity modes, since there is only one lasing steady state in the system with optoelectronic feedback. The threshold condition $N(t) > 0$ is fulfilled when $D(t) > 0$, which results in a small laser pulse having intensity $I_C(t)$ of four order magnitude less than the multiplet pulses. The small pulse is visible in the zoomed-in

intensity time trace of the triplet, Fig. 3(b). The pulse lags behind the triplet because of the small $D(t)$ value, which determines a relatively large turn-on delay of the small pulse. With the pump parameter increased, the large amplitude triplet becomes unstable, and the large amplitude quadruplet becomes stable when the small pulse rapidly grows into a new full-amplitude pulse (Fig. 3(c)), as discussed below. The location of the added large-amplitude pulse in the multiplet structure is predetermined by the time slot of $D(t) > 0$, as shown by an arrow in Fig. 3.

Let us analyze the pulse-adding evolution of the multiplets using a 2D diagram[35] in Fig. 4. The diagram is built from the time series, and shows the evolution of the dynamics from roundtrip to roundtrip when the pump parameter is increased in a step-wise manner per $\Delta P = 0.0005$ every period of 1000τ. In Fig. 4, the triplet (corresponding to Fig. 3(a,b)) loses its stability at $P = -0.0085$ and the small last pulse grows resulting in the quadruplet (corresponding to Fig. 3(c)), with the fourth large pulse position becoming closer to the main group. With the further pump increase, the quadruplet transforms into quintuplet, that, after another pump rise, changes into the equally-spaced pulse train at the sixth harmonic of f_τ pulses. We emphasize that some stable multiplets in Fig. 4 may coexist and the stable singlet coexists with all of them up until $P = -0.0075$.

We summarize that there are two key stages in the formation of multiplets: i) localized overshoot in the $D(t)$ signal caused by ringing due to the high-pass filtering of the electrical feedback signal which results in the small amplitude laser intensity pulse; ii) rapid growth of the small amplitude pulse into a high amplitude pulse of the multiplet. Experimental and theoretical multiplets show the interpulse time to decrease and then to increase through the burst which is typical for parabolic bursters[36]. An open question is then whether the spike-adding process in the present system is similar to the spike-adding explosive process occurring in certain slow-fast dynamical systems with parabolic bursting which have been previously heuristicaly described in the neuromorphic context[37].

To conclude, in this work, we have reported on a cascade of multiplets in a semiconductor laser subject to nonlinear optoelectronic feedback. Multiplets are observed in the vicinity of the lasing threshold, and therefore demonstrate gain-switching character. Multiplet structures can be formed by either equidistant or non-equidistant intensity pulses with identical profiles and are strongly dependent on the cut-off frequency filtering properties of the feedback loop. Higher numbers of pulses per multiplet are observed experimentally when the pump current is increased. This scenario is confirmed by the modeling in good agreement with the experiment. Our work demonstrates a relatively simple feedback laser configuration designed to generate and control bursting multiplet intensities which are of interest for various applications from lidar to neuromorphic studies.

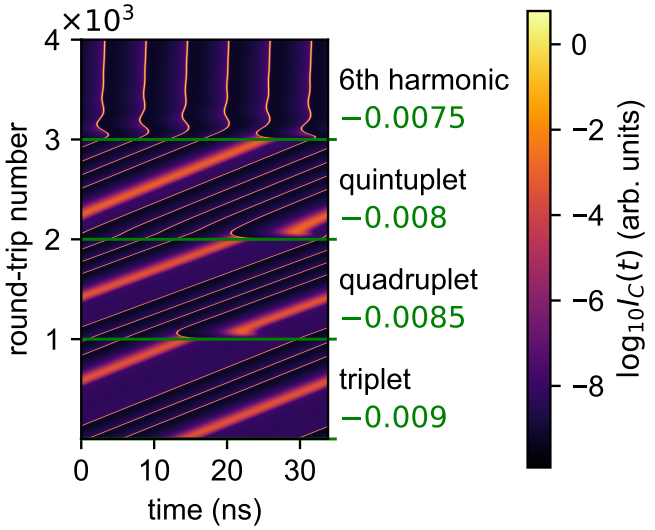

FIG. 4. Two-dimensional diagram of the multiplet regime evolution computed theoretically when the pump parameter increases, showing the following scenario: triplet → quadruplet → quintuplet → the sixth harmonic of $1/\tau$ pulses. The horizontal axis represents a single roundtrip, and the vertical is the number of the roundtrips. Color shows the intensity that is given in a logarithmic scale, for clarity. The feedback strength $\eta = 0.00129$, the pump parameter P was increased by steps of $\Delta P = 0.0005$ every 1000τ, and its values are denoted in green. The other parameters are given in the text.

ACKNOWLEDGMENT

The work of A.V.K., G.O.D., and E.A.V. was supported by the Ministry of Science and Higher Education of the Russian Federation, research Project No. 2019-1442 (Project Reference No. FSER 2020-0013). A.L., D.S.C., and M.S.I. acknowledge the financial support of the Conseil Régional Grand Est.

DATA AVAILABILITY

The data that support the findings of this study are available from the corresponding author upon reasonable request.

[1] E. M. Izhikevich, *Dynamical systems in neuroscience* (MIT press, 2007).
[2] R. Knappe, H. Haloui, A. Seifert, A. Weis, and A. Nebel, "Scaling ablation rates for picosecond lasers using burst micromachining," in *Laser-based Micro-and Nanopackaging and Assembly IV*, Vol. 7585 (SPIE, 2010) pp. 150–155.
[3] H. Le, T. Karkantonis, V. Nasrollahi, P. Penchev, and S. Dimov, "Mhz burst mode processing as a tool for achieving removal rates scalability in ultra-short laser micro-machining," Applied Physics A **128**, 711 (2022).
[4] V. Belloni, V. Sabonis, P. Di Trapani, and O. Jedrkiewicz, "Burst mode versus single-pulse machining for bessel beam micro-drilling of thin glass: Study and comparison," SN Applied Sciences **2**, 1–12 (2020).
[5] S. T. Hendow, R. Romero, S. A. Shakir, and P. T. Guerreiro, "Percussion drilling of metals using bursts of nanosecond pulses," Optics express **19**, 10221–10231 (2011).
[6] M. N. Slipchenko, J. D. Miller, S. Roy, J. R. Gord, S. A. Danczyk, and T. R. Meyer, "Quasi-continuous burst-mode laser for high-speed planar imaging," Optics Letters **37**, 1346–1348 (2012).

[7]E. Wachter and W. Fisher, "Coherent-burst laser ranging: decoupling resolution and unambiguous range," Optics letters **22**, 570–572 (1997).
[8]J.-H. Hung, H.-J. Yan, K. Sato, H. Yamada, L.-H. Peng, and H. Yokoyama, "Optical burst pulse generation from a gain-switched laser diode through cw laser light injection," in *Conference on Lasers and Electro-Optics/Pacific Rim* (Optica Publishing Group, 2018) pp. W3A–36.
[9]B. Kelleher, B. Tykalewicz, D. Goulding, N. Fedorov, I. Dubinkin, T. Erneux, and E. A. Viktorov, "Two-color bursting oscillations," Scientific Reports **7**, 8414 (2017).
[10]M. Marconi, J. Javaloyes, S. Balle, and M. Giudici, "How lasing localized structures evolve out of passive mode locking," Physical review letters **112**, 223901 (2014).
[11]S. Terrien, V. A. Pammi, B. Krauskopf, N. G. Broderick, and S. Barbay, "Pulse-timing symmetry breaking in an excitable optical system with delay," Physical Review E **103**, 012210 (2021).
[12]S. Tarucha and K. Otsuka, "Response of semiconductor laser to deep sinusoidal injection current modulation," IEEE Journal of Quantum Electronics **17**, 810–816 (1981).
[13]X. S. Yao and L. Maleki, "High frequency optical subcarrier generator," Electronics Letters **30**, 1525–1526 (1994).
[14]M. J. Wishon, D. Choi, T. Niebur, N. Webster, Y. K. Chembo, E. A. Viktorov, D. Citrin, and A. Locquet, "Low-noise x-band tunable microwave generator based on a semiconductor laser with feedback," IEEE Photonics Technology Letters **30**, 1597–1600 (2018).
[15]W. Weng, A. Kaszubowska-Anandarajah, J. He, P. D. Lakshmijayasimha, E. Lucas, J. Liu, P. M. Anandarajah, and T. J. Kippenberg, "Gain-switched semiconductor laser driven soliton microcombs," Nature communications **12**, 1425 (2021).
[16]T. Damen and M. Duguay, "Optoelectronic regenerative pulser," Electronics Letters **16**, 166–167 (1980).
[17]M. S. Islam, A. Kovalev, G. Coget, E. Viktorov, D. Citrin, and A. Locquet, "Staircase dynamics of a photonic microwave oscillator based on a laser diode with delayed optoelectronic feedback," Physical Review Applied **13**, 064038 (2020).
[18]P. Munnelly, B. Lingnau, M. M. Karow, T. Heindel, M. Kamp, S. Höfling, K. Lüdge, C. Schneider, and S. Reitzenstein, "On-chip optoelectronic feedback in a micropillar laser-detector assembly," Optica **4**, 303–306 (2017).
[19]Y. K. Chembo, D. Brunner, M. Jacquot, and L. Larger, "Optoelectronic oscillators with time-delayed feedback," Rev. Mod. Phys. **91**, 035006 (2019).
[20]S. Tang and J. Liu, "Chaotic pulsing and quasi-periodic route to chaos in a semiconductor laser with delayed opto-electronic feedback," IEEE journal of quantum electronics **37**, 329–336 (2001).
[21]H. D. Abarbanel, M. B. Kennel, L. Illing, S. Tang, H. Chen, and J. Liu, "Synchronization and communication using semiconductor lasers with optoelectronic feedback," IEEE journal of quantum electronics **37**, 1301–1311 (2001).
[22]F.-Y. Lin and J.-M. Liu, "Nonlinear dynamics of a semiconductor laser with delayed negative optoelectronic feedback," IEEE journal of quantum electronics **39**, 562–568 (2003).
[23]F. Lin and J. Liu, "Harmonic frequency locking in a semiconductor laser with delayed negative optoelectronic feedback," Applied physics letters **81**, 3128–3130 (2002).
[24]G.-Q. Xia, S.-C. Chan, and J.-M. Liu, "Multistability in a semiconductor laser with optoelectronic feedback," Optics Express **15**, 572–576 (2007).
[25]M. S. Islam, A. V. Kovalev, E. A. Viktorov, D. S. Citrin, and A. Locquet, "Optical square-wave generation in a semiconductor laser with optoelectronic feedback," Opt. Lett. **46**, 6031–6034 (2021).
[26]H. Tian, L. Zhang, Z. Zeng, W. Lyu, Z. Fu, Z. Xu, Z. Zhang, Y. Zhang, S. Zhang, H. Li, and Y. Liu, "Neuromorphic regenerative memory optoelectronic oscillator," Opt. Express **31**, 27529–27542 (2023).
[27]M. Hejda, J. Robertson, J. Bueno, J. A. Alanis, and A. Hurtado, "Neuromorphic encoding of image pixel data into rate-coded optical spike trains with a photonic VCSEL-neuron," APL Photonics **6**, 060802 (2021), https://pubs.aip.org/aip/app/article-pdf/doi/10.1063/5.0048674/16735181/060802_1_online.pdf.
[28]J. Busck and H. Heiselberg, "Gated viewing and high-accuracy three-dimensional laser radar," Appl. Opt. **43**, 4705–4710 (2004).
[29]T. Chen, H. Liu, W. Kong, and R. Shu, "Burst-mode-operated, sub-nanosecond fiber mopa system incorporating direct seed-packet shaping," Opt. Express **24**, 20963–20972 (2016).
[30]M. S. Islam, A. V. Kovalev, E. A. Viktorov, D. S. Citrin, and A. Locquet, "Microwave Frequency Comb Generation by Gain-Switching Versus Relaxation Oscillations," IEEE Photonics Technology Letters **33**, 491–494 (2021).
[31]K. Y. Lau and A. Yariv, "Self-sustained picosecond pulse generation in a GaAlAs laser at an electrically tunable repetition rate by optoelectronic feedback," Applied Physics Letters **45**, 124–126 (1984).
[32]K. Y. Lau, "Gain switching of semiconductor injection lasers," Appl. Phys. Lett. **52**, 257–259 (1988).
[33]C. Yan, K. P. Reddy, R. K. Jain, and J. G. McInerney, "Picosecond Pulse Generation in CW Semiconductor Lasers Using a Novel Regenerative Gain-Switching Technique," IEEE Photon. Technol. Lett. **5**, 494–497 (1993).
[34]H. Erzgräber, D. Lenstra, B. Krauskopf, A. Fischer, and G. Vemuri, "Feedback phase sensitivity of a semiconductor laser subject to filtered optical feedback: Experiment and theory," Physical Review E **76**, 026212 (2007).
[35]G. Giacomelli and A. Politi, "Relationship between delayed and spatially extended dynamical systems," Phys. Rev. Lett. **76**, 2686–2689 (1996).
[36]G. B. Ermentrout and N. Kopell, "Parabolic Bursting in an Excitable System Coupled With a Slow Oscillation." (1986).
[37]M. Desroches, M. Krupa, and S. Rodrigues, "Spike-adding in parabolic bursters: The role of folded-saddle canards," Physica D: Nonlinear Phenomena **331**, 58–70 (2016).